JOURNAL OF MATERIALS SCIENCE 36 (2001) 5575–5580

Effect of chromium on the corrosion behavior of iron aluminides in thiosulfate-chloride solution

YOON-SEOK CHOI, SEUNG-HO AHN, JUNG-GU KIM,
Department of Advanced Materials Engineering, Sung Kyun Kwan University, 300 Chunchun-Dong, Jangan-Gu, Suwon 440-746, Korea
E-mail: kingo@chollian.net

C. G. McKAMEY
Metals and Ceramics Division, Oak Ridge National Laboratory, Oak Ridge, TN 37831-6115, USA

Aqueous corrosion characteristics of iron aluminides in thiosulfate-chloride solution were studied as a function of chromium addition. Four kinds of iron aluminides, namely, FA-61, FA-77, FA-72 and FA-78, were prepared by arc melting followed by thermomechanical treatment. The corrosion behavior in thiosulfate-chloride solution for the prepared alloys were investigated by electrochemical tests (potentiodynamic test, potentiostatic test and electrochemical impedance spectroscopy (EIS) measurement) and surface analyses. The results of the potentiodynamic test indicated that the breakdown potential increased with increasing Cr content. Cr additions were found to prevent passive film from undergoing pitting corrosion. In EIS measurement, the depression angle was inversely related to pitting resistance, and decreased with increasing chromium content. The SEM observations of the sample surfaces reveal the different forms of pit as a function of chromium content. The AES results give evidence that the thiosulfate ions are reduced on the metallic surface, which inhibits the repassivation process.

1. Introduction

Intermetallic alloys are one of the most interesting new classes of metallic materials by virtue of their superior characteristics. For example, the ordered intermetallic iron aluminides represent attractive candidates for high temperature applications because they have excellent oxidation and sulfidation resistances at high temperatures due to protective aluminum oxide (Al_2O_3) scales [1]. Another strong point of iron aluminides is their low density ($\rho = 6.6$ g/cm^3) compared to steels ($\rho = 7.8$ g/cm^3) and nickel-based alloys ($\rho = 8.5$ g/cm^3).

However, the major limitations of these materials are their low ductility at room temperatures and a sharp drop in mechanical strength above 600°C [2]. These properties can be improved by adding ternary elements such as Cr, Mo, and Mn [3–5].

Iron aluminides have a wide range of uses where more expensive stainless steels and nickel-based alloys are being used (e.g., automobile exhaust system, gas clean-up system, and fossil energy production area in sulfur-bearing environments). In these environments, thiosulfate anions may be present with chloride ions. It was proved that these species exert a detrimental influence on the pitting behavior of Fe-Cr-Ni alloys [6]. Furthermore, in sodium chloride solution with the addition of sodium thiosulfate, enhanced pitting corrosion as compared with that found in pure sodium chloride solution was reported [7]. Although thiosulfate anions alone have not been found aggressive enough to cause damage to stainless steel, they have been shown to act in synergy with other common ions, such as chlorides to cause severe localized corrosion [8].

In order to increase the application of iron aluminides, it is important to evaluate their aqueous corrosion properties in a sulfur-bearing environment.

The purpose of this research is to investigate the effect of chromium on the corrosion characteristics of the iron aluminides in thiosulfate-chloride solution. Electrochemical methods and surface analysis techniques were used to determine the pitting resistance of iron aluminides.

2. Experimental procedure

2.1. Materials and preparation

Alloy specimens of 500 g were prepared by arc-melting the constituent elements in a water-cooled copper crucible in a chamber backfilled with argon. The specimens were remelted six times for homogeneity and then were drop cast into a copper mold to form ingots. The ingots were hot-forged 50% at 1,000°C, hot-rolled 50% at 800°C, and warm-rolled 70% at 650°C to a final thickness of 0.75 mm. Chemical compositions of the iron aluminides (at.%) used for experiments are given in Table I. Heat treatment was stress relieving at 750°C for 1 hour, followed by an oil quench, which produced the B2-ordered structure.

TABLE I Chemical compositions of iron aluminides (at.%)

Material	Fe	Al	Cr
FA-61	72	28	0
FA-77	70	28	2
FA-72	68	28	4
FA-78	66	28	6

2.2. Electrolytes

It was suggested earlier that the ratio of chloride to thiosulfate concentration would control the occurrence of pitting as the overall ionic strength is valid [9, 10]. In the present study, an aerated thiosulfate-chloride solution was used to simulate a sulfur-bearing environment. The chloride-thiosulfate ratio was 5 (Chloride 50 ppm/thiosulfate 10 ppm). Solution was aerated with pure air at a flow rate of 10 cc/min.

2.3. Investigation methods

Electrochemical polarization of the sample was accomplished with an EG & G Model 273A Potentiostat. The potentiostat was programmed to apply a continuously varying potential to the sample at a rate of 600 mV/h. Each specimen was mounted in epoxy that was cured in an air for 24 h. The specimen was finished by grinding on 600-grit silicon carbide paper. To prevent the initiation of crevice corrosion between the epoxy and the speciment, the epoxy-specimen interface was painted with Amercoat 90 epoxy, leaving an exposed area of 1 cm^2 on the material surface.

All potentials were measured against the saturated calomel electrode (SCE). For each material and electrolyte combination, the corrosion sample was allowed to stabilize in the electrolyte, until the potential change was $<$1mV/min. This potential then was taken as the open-circuit potential(OCP). To insure reproducibility, at least three replicates were run for each specimen.

The potentiostatic tests were performed to examine the tendency of passivation and break down (pit propagation) as a function of Cr content. After each potentiostatic test, electrochemical impedance spectroscopy(EIS) measurements were investigated to compare the impedance behavior between passivation and breakdown state. EIS instrumentation consisted of a EG&G Model 273A potentiostat and Model 1025 frequency response detector controlled by Model 398 electrochemical impedance software. EIS measurements were performed in the frequency range between 10 kHz and 10 mHz. Sinusoidal voltage of $\pm$5 mV was supplied and DC potential was set to corrosion potential.

To investigate the relationship between the anodic behavior and surface morphology of pitting, the surface was examined by SEM after EIS measurement. Elemental concentration profiles through the passive films and pits were obtained using Auger electron spectroscopy (AES) in conjunction with argon ion sputtering. A Perkin-Elmer Physical Electronics Model PHI 680 was used for AES analyses. The sputter rate was calibrated to 82 Å/min on SiO_2.

3. Results and discussion

The anodic polarization curves of the four iron aluminides are presented in Fig. 1. All the alloys passivated

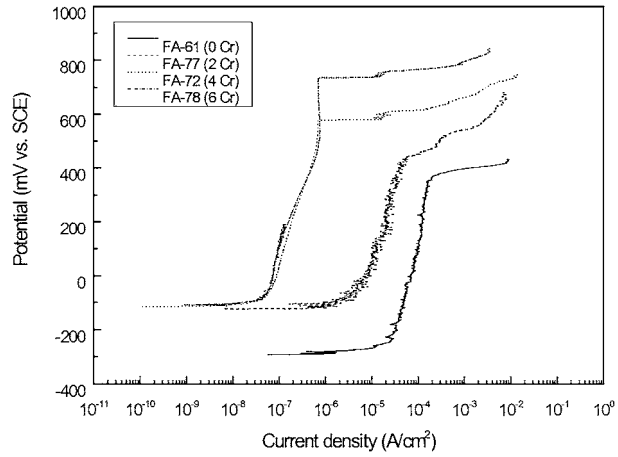

Figure 1 Anodic polarization curves of iron aluminides in thiosulfate-chloride solutions.

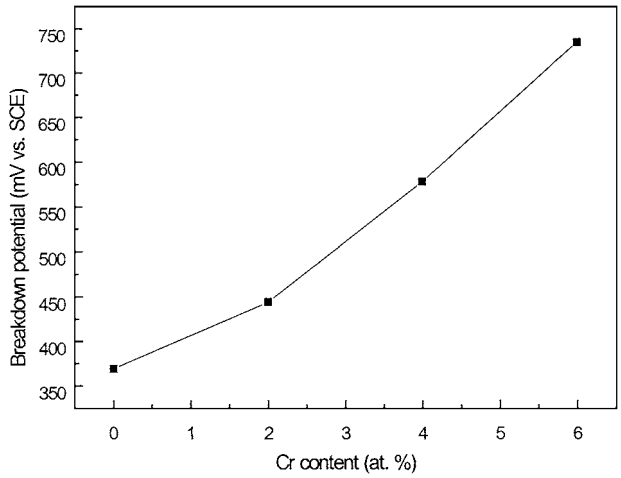

Figure 2 Effect of Cr content on the breakdown potential.

in these thiosulfate-chloride solutions. However, polarization above the breakdown potential resulted in a marked increase in current density as the result of the initiation of pitting. Fig. 2 shows the effect of chromium addition on the breakdown potential. The breakdown potential increased with increasing chromium content, indicating increased relative resistance to initiation of localized corrosion. The passive current densities are shown to be decreased by increasing Cr content, which was a result of more stable passive film on the surface.

Fig. 3 shows Nyquist impedance plots of iron aluminides in passive state after potentiostatic test at applied anodic potential of 100 mV_{SCE} for 1 hour. The applied anodic potential results in passive films that create dramatic increase in impedance. Addition of chromium had no effect on the behavior at passivation state. This indicates that the corrosion reactions are not controlled by the chromium compound, but must be controlled by the iron or aluminum compound. The capacitive impedance appears to be related to the formation of the adherent passive film [11].

Fig. 4 shows the result of potentiostatic tests performed at an applied potential of +735 mV_{SCE}. The applied potential was based on the data from polarization curves in Fig. 1, corresponding to the breakdown potential of FA-78. The current density increased and

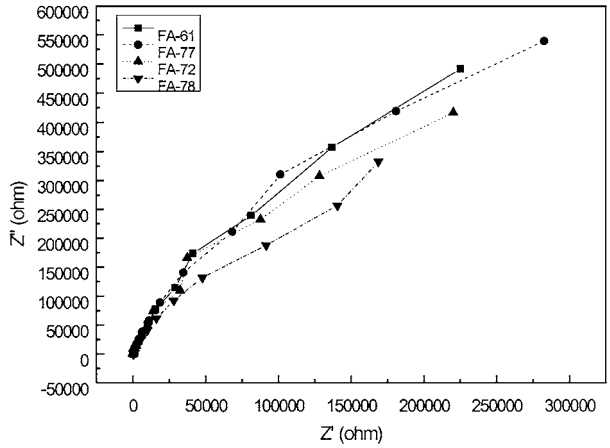

Figure 3 Nyquist plots for iron aluminides at passivation state.

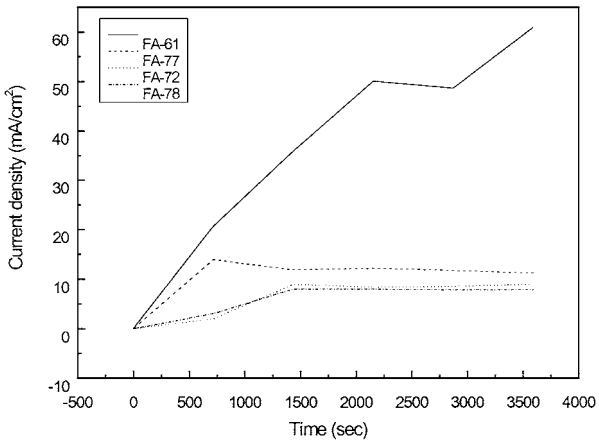

Figure 4 Current variation with time at a breakdown potential of +735 mV_{SCE}.

then it remained almost constant through the experiment except for FA-61. The current density for FA-78 and FA-72 decreased slowly with time, implying that the addition of chromium to iron aluminides increased the resistance to pitting corrosion. The increased current density would be directly related to the pit initiation and propagation.

Fig. 5 shows Nyquist plots of iron aluminides after potentiostatic test at a constant potential of 735 mV_{SCE} for 1 hour. The impedance spectra obtained at breakdown state are different from those at passivation state.

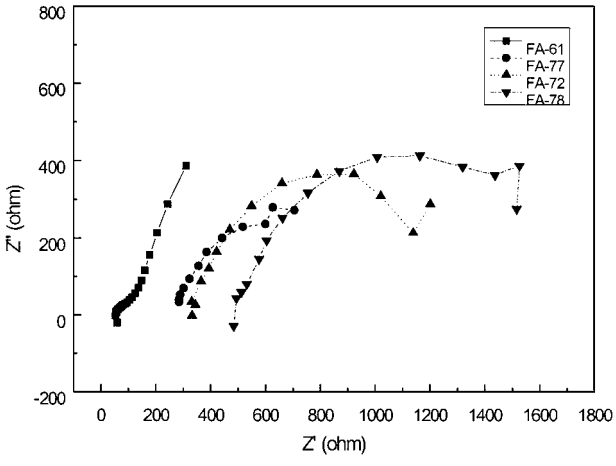

Figure 5 Nyquist plots for iron aluminides at breakdown state.

TABLE II Analyzed EIS measurements at breakdown state

Material	R_s (Ω)	R_p (Ω)	E_B (mV_{SCE})	Depression angle (deg)
FA-61	52.7	202.5	369	−32.6
FA-77	280.2	778.7	443	−21.7
FA-72	329.9	1,108	578	−19.4
FA-78	491	1,249	735	−19.4

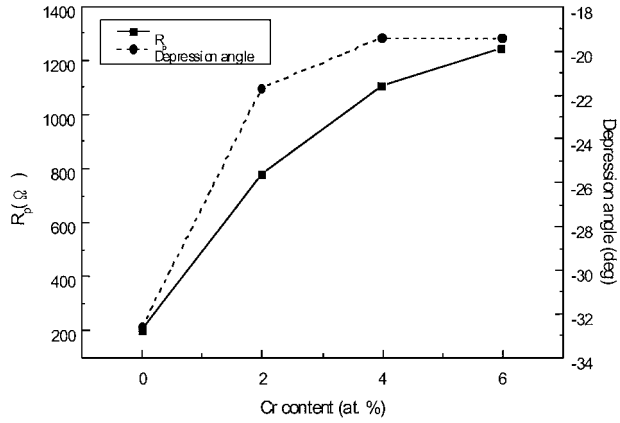

Figure 6 Correlation between calculated depression angles and polarization resistance as a function of Cr content.

The diameter of arc increased with Cr content. The increase in diameter of the arc indicated an increase in the R_p value. Such an increase in R_p is attributed to a stable and protective passive film on the surface. It was normal to extrapolate that the surface modifications, introduced by the formation and propagation of localized pits, should be somewhat related to the calculated depression angle [12]. Table II and Fig. 6 represent an attempt that was made to correlate both R_p and depression angle as a function of chromium content. Good correlation was obtained between R_p and depression angle shown in Fig. 6. It was suggested that the depression angle was inversely related to pitting resistance, and decreased with increasing chromium content. It was also observed that the R_s value increased with increasing chromium content as shown in Table II. The increased R_s value is due to the decreased anodic dissolution rate. In the case of FA-61, it was found that the diffusion tail appears on the low frequency portion. When a diffusion tail was present, it is necessary to assume that there was rapid exchange of metal cations among the metal, the pit and the solution, with the diffusion tail arising from the diffusion of the metal cations in solution.

Fig. 7 shows the scanning electron micrographs of pitting after the potentiostatic tests at the breakdown potential. Many pits, caused by $S_2O_3^{2-}$ and Cl^- were formed on FA-61, and the number of pits was reduced for FA-77, and few pits on FA-72 and FA-78. The size and the number of pits decreased with increasing chromium content.

It is generally accepted that the pit morphology depends on whether the process is activation or diffusion controlled. When diffusion predominates, the hemispherical pits formed on surface [13]. In FA-61 not containing Cr, a large number of hemispherical shaped pits formed on the grains have been detected. This

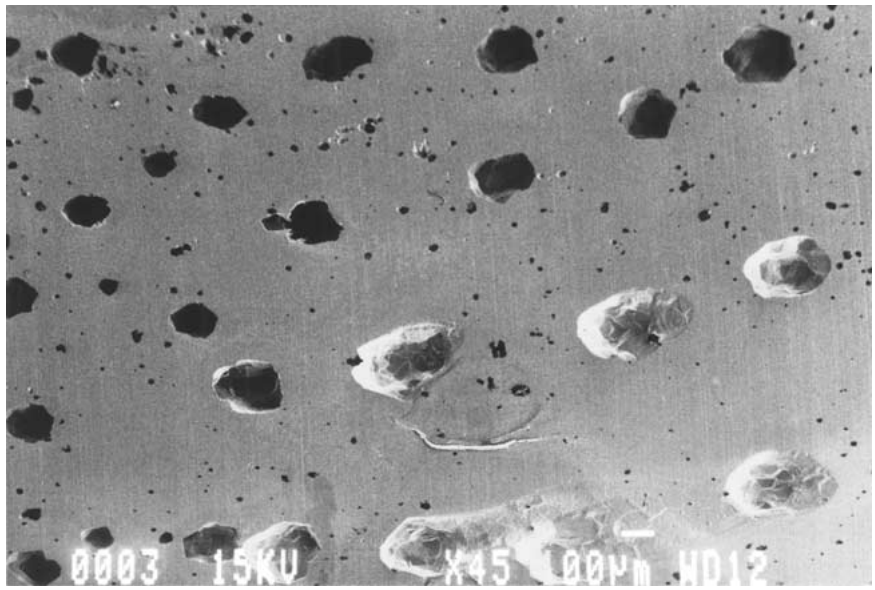

(a)

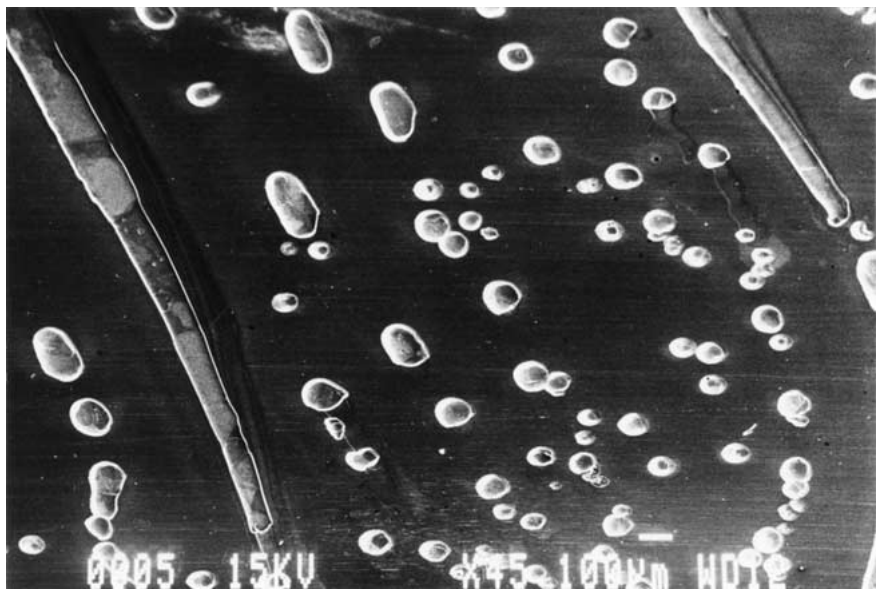

(b)

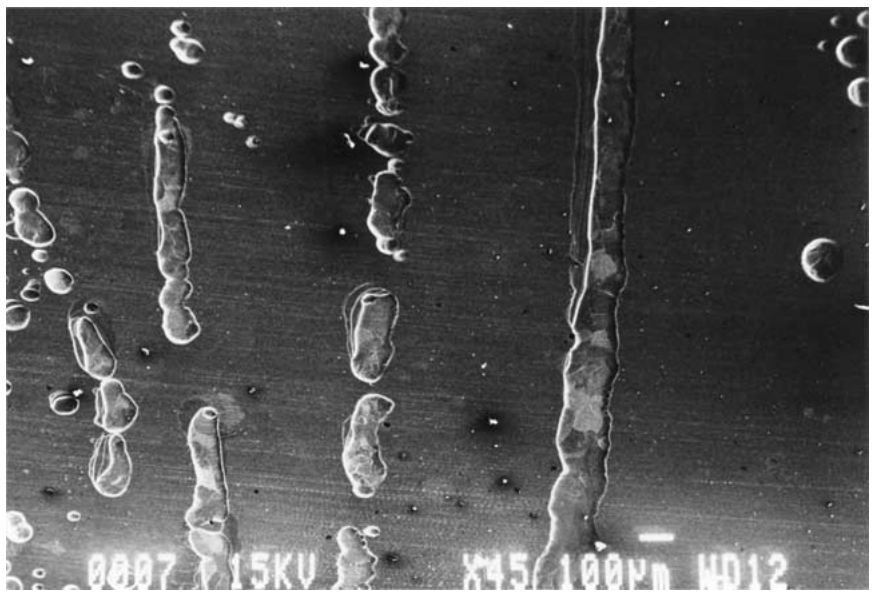

(c)

Figure 7 Surface morphologies of pitting: (a) FA-61, (b) FA-77, (c) FA-72 and (d) FA-78. (*Continued*.)

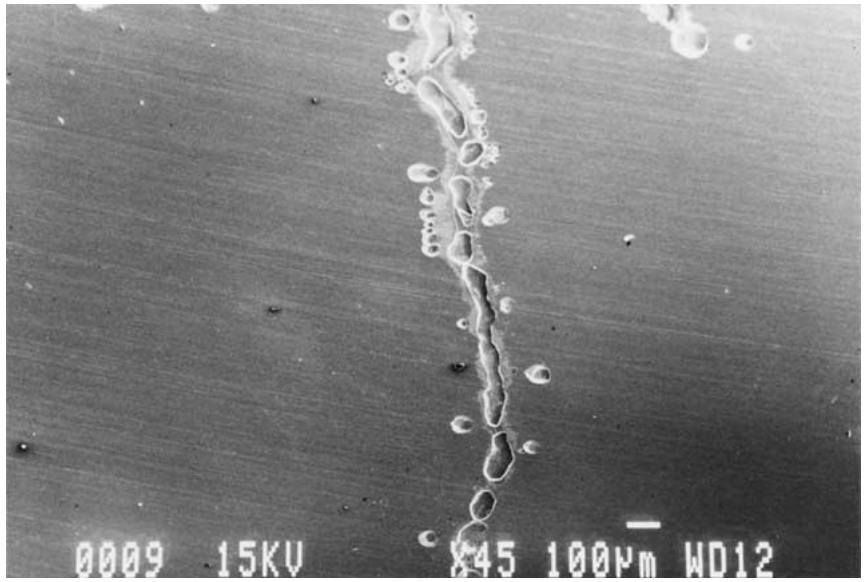

(d)

Figure 7 (*Continued*).

result indicated that the diffusion tail appeared in EIS measurement, and was correlated to the pitting process. When the chromium was added, however, the numbers of pits were greatly reduced and it was accompanied by a transformation from hemispherical to irregular tunneling attack morphology. This result supports that the chromium contributes to a modification of pit propagation mechanism. In other words, when the chromium is absent, the pits grow in depth, whereas in the presence of chromium, the pits grow in length.

Fig. 8 presents the results of an AES analyses of the pits and surfaces of iron aluminides obtained from the specimens after the potentiostatic tests at the breakdown potential and shows their in-depth profiles of Cr contents. The Cr content of FA-78 was more enriched in the surface films than those of FA-72 and FA-77. This means that the chromium enrichment inside the pit and passive film on alloys contributes to an increased resistance to pit propagation.

AES analyses also detected sulfur species on the pits and surfaces of specimens (Fig. 9). The results give the evidence that the thiosulfates are reduced to absorbed sulfur, which inhibits the repassivation process once pitting has initiated. The sequence of reaction is explained as following [14, 15]. At first, $S_2O_3^{2-}$ was oxidized to form S by the following reaction.

$$S_2O_3^{2-} + H^+ \Rightarrow S + HSO_3^-$$

S was further oxidized and incorporated with H^+ according to the following reaction.

$$S + 2H^+ + 2e \Rightarrow H_2S$$

It was possible that the pre-existing metal oxide reacted with H_2S to form sulfide in accordance with the following reaction.

$$MO + H_2S \Rightarrow MS + H_2O$$

After sputtering, sulfur species disappeared. This means that the absorbed sulfur species layer was thin. However, the absorbed depth of sulfur species was different as a function of chromium content. In FA-61 not

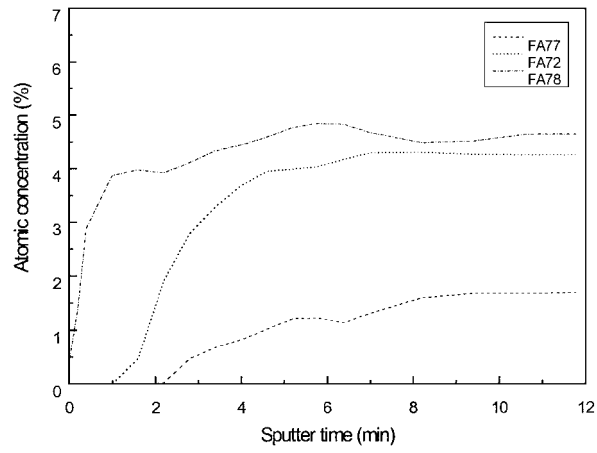

(a)

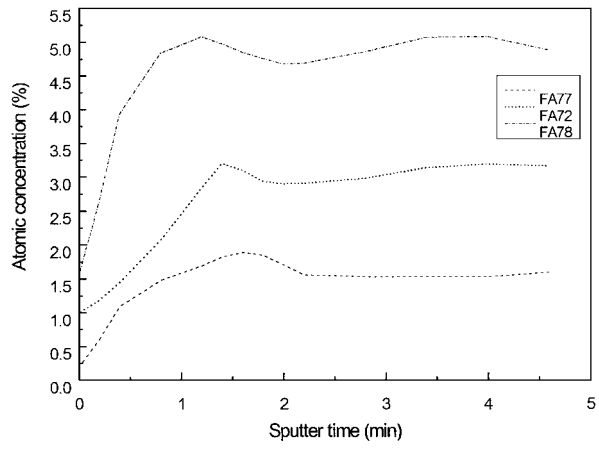

(b)

Figure 8 Depth profiling of Cr on iron aluminides after potentiostatic test: (a) Inside of pit and (b) passivated surface.

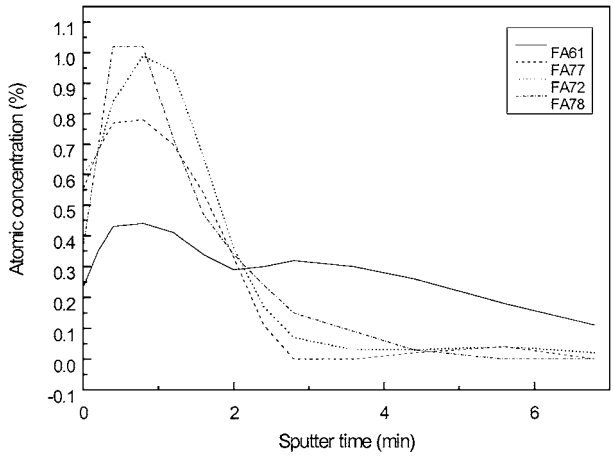

Figure 9 Depth profiling of S on iron aluminides after potentiostatic test.

containing Cr, the depth was about 1,246 Å, while the chromium is added the depth was about 328 Å. This indicated that the addition of chromium prevents the penetration of sulfur species into metal surface owing to the formation of passive film. These results provide a good interpretation for the above mentioned pit propagation mechanism.

4. Conclusions

1. Cr additions increased the breakdown potential and decreased the passive current density, indicating increased resistance to initiation of pitting corrosion

2. The relationship between R_p and depression angle from EIS measurement suggested that the depression angle was inversely related to pitting resistance (i.e., the depression angle decreased with increasing chromium content).

3. The observation of surface morphology after corrosion tests showed that the iron aluminides containing chromium had far fewer pits than that containing no chromium. The modification in pit shape indicated that the pitting process was changed by chromium addition from diffusion control to activation control in this thiosulfate-chloride solution.

4. The presence of sulfur species on the corroded surface indicated that the thiosulfates are reduced to absorbed sulfur, which inhibits the repassivation process. And the penetration depth of the absorbed sulfur species decreased with chromium addition.

References

1. C. G. McKAMEY and J. H. DEVAN, *Mater. Sci. Eng.* **A153** (1992) 573.
2. C. G. McKAMEY, J. H. DEVAN, P. F. TORTORELLI and V. K. SIKKA, *J. Mater. Res.* **6** (1991) 1779.
3. C. G. McKAMEY, J. A. HOUSTON and C. T. LIU, *ibid.* **4** (1989) 1156.
4. C. G. McKAMEY and C. T. LIU, *Scripta Metall. Mater.* **24** (1990) 2119.
5. D. G. MORRIS, M. M. DADRAS and M. A. MORRIS, *Acta Metall. Mater.* **41** (1993) 97.
6. J. GUTZEIT, in "Process Industries Corrosion," edited by B. J. MONIZ and W. I. POLLOCK (NACE, Houston, TX. 1987) p. 171.
7. R. ROBERGE, *Corrosion* **44** (1988) 274.
8. R. C. NEWMAN, *ibid.* **41** (1985) 450.
9. A. GARNER, *ibid.* **41** (1985) 587.
10. J. O. PARK, M. VERHOFF and R. ALKIRE, *Electrochimica Acta* **42** (1997) 3281.
11. H. HACK and H. PICKERING, in "Electrochemical Impedance: Analysis and Interpretation," edited by J. R. SCULLY, D. C. SILVERMAN and M. W. KENDIG (ASTM STP 1188, ASTM, Philadelphia, PA. 1993) p. 220.
12. P. R. ROBERGE, E. HALLIOP and V. S. SASTRI, *Corrosion* **48** (1992) 447.
13. N. DE CRISTOFARO, S. FRANGINI and A. MIGNONE, *Corrosion Sci.* **38** (1996) 307.
14. C. DURET-THUAL, D. COSTA, W. P. YANG and P. MARCUS, *ibid.* **39** (1997) 913.
15. H. S. KUO, H. CHANG and W. T. TSAI, *ibid.* **41** (1999) 669.

Received 20 October 2000
and accepted 13 August 2001